

127

ADA 041920

A Solid Friction Model

20000726107

Prepared by P. R. DAHL

May 1968

DDC
JUL 22 1977
C

Prepared for
SPACE AND MISSILE SYSTEMS ORGANIZATION
AIR FORCE SYSTEMS COMMAND
Los Angeles Air Force Station
P.O. Box 92960, Worldway Postal Center
Los Angeles, Calif. 90009

Contract No. AF04095-67-C-0158



THE AEROSPACE CORPORATION

APPROVED FOR PUBLIC RELEASE:
DISTRIBUTION UNLIMITED

Reproduced From
Best Available Copy


AD NO. 1
DDC FILE COPY

This report was submitted by The Aerospace Corporation, El Segundo, CA 90245, under Contract AF04695-67-C-0158 with the Space and Missile Systems Organization (AFSC), Los Angeles Air Force Station, P. O. Box 92960, Worldway Postal Center, Los Angeles, CA 90009. Lieutenant A. G. Fernandez, YAPT was the Deputy for Advanced Space Programs project officer.

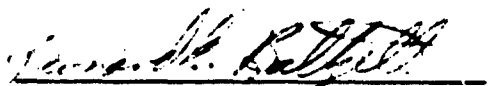
This report has been reviewed by the Information Office (OI) and is releasable to the National Technical Information Service (NTIS). At NTIS, it will be available to the general public, including foreign nations.

This technical report has been reviewed and is approved for publication. Publication of this report does not constitute Air Force approval of the report's findings or conclusions. It is published only for the exchange and stimulation of ideas.


A. G. Fernandez, 1st Lt, YAPT
Project Engineer


Joseph Gassmann, Maj, USAF

FOR THE COMMANDER


Leonard E. Baltzell, Col, USAF
Asst. Deputy for Advanced Space
Programs

UNCLASSIFIED

SECURITY CLASSIFICATION OF THIS PAGE (When Data Entered)

REPORT DOCUMENTATION PAGE		READ INSTRUCTIONS BEFORE COMPLETING FORM	
1. REPORT NUMBER SAMS0 TR-77-131 ✓	2. GOVT ACCESSION NO.	3. RECIPIENT'S CATALOG NUMBER	
4. TITLE (and Subtitle) A SOLID FRICTION MODEL, ✓	5. TYPE OF REPORT & PERIOD COVERED Technical rept, ✓	6. PERFORMING ORG. REPORT NUMBER TOR-0158(3107-18)-1 ✓	
7. AUTHOR(s) P. R./Dahl ✓	8. CONTRACT OR GRANT NUMBER(s) F04695-67-C-0158 ✓	9. PERFORMING ORGANIZATION NAME AND ADDRESS The Aerospace Corporation El Segundo, Calif. 90245	
10. PROGRAM ELEMENT, PROJECT, TASK AREA & WORK UNIT NUMBERS	11. CONTROLLING OFFICE NAME AND ADDRESS 1234p. ✓	12. REPORT DATE May 1968 ✓	
13. MONITORING AGENCY NAME & ADDRESS (if different from Controlling Office) Space and Missile Systems Organization Air Force Systems Command Los Angeles, Calif. 90009	14. NUMBER OF PAGES 28	15. SECURITY CLASS. (of this report) Unclassified	
15a. DECLASSIFICATION/DOWNGRADING SCHEDULE			
16. DISTRIBUTION STATEMENT (of this Report) Approved for public release; distribution unlimited			
17. DISTRIBUTION STATEMENT (of the abstract entered in Block 20, if different from Report)			
18. SUPPLEMENTARY NOTES			
19. KEY WORDS (Continue on reverse side if necessary and identify by block number) Solid Friction Friction Sliding Friction Coulomb Friction			
20. ABSTRACT (Continue on reverse side if necessary and identify by block number) A model is developed for sliding and rolling friction that can be used in simulations of dynamic systems involving mechanical elements that are subject to friction. Sound bases for the model are developed around the hypothesis that the origin of friction is in quasi static contact bonds that are continuously formed and subsequently broken. Sliding friction, including coulomb friction and the so-called "stiction," as well as rolling friction are believed to be realistically simulated by the model. The OVER			

DDC
JUL 22 1968

DD FORM 1473 (FACSIMILE)

009500

UNCLASSIFIED
SECURITY CLASSIFICATION OF THIS PAGE (When Data Entered)

41

UNCLASSIFIED

SECURITY CLASSIFICATION OF THIS PAGE(When Data Entered)

19. KEY WORDS (Continued)

20. ABSTRACT (Continued)

model has been proven to accurately simulate transient torque and rate measurements on ball bearings tested in the laboratory.

ADVISORY	
NTIS	Write Section <input checked="" type="checkbox"/>
DIC	Ref Section <input type="checkbox"/>
UNANNOUNCED	<input type="checkbox"/>
JUSTIFICATION.....	
.....	
437	
DISTRIBUTION/AVAILABILITY CODES	
844	AVAIL. CODE OR SPECIAL
A	

UNCLASSIFIED

SECURITY CLASSIFICATION OF THIS PAGE(When Data Entered)

A SOLID FRICTION MODEL

**Prepared by
P. R. Dahl**

May 1968

**THE AEROSPACE CORPORATION
El Segundo, Calif. 90245**

**Prepared for
SPACE AND MISSILE SYSTEMS ORGANIZATION
AIR FORCE SYSTEMS COMMAND
LOS ANGELES AIR FORCE STATION
P.O. Box 92960, Worldway Postal Center
Los Angeles, Calif. 90009**

Contract No. AF04695-67-C-0158

**Approved for public release;
distribution unlimited**

A SOLID FRICTION MODEL

Prepared by

P. H. Campbell (for)
P. R. Dahl
GE Project Office

for L.W. Inge
R. W. Rector
Management Systems Office

Approved

J. R. Henry (for)
J. R. Henry, Director
GE Project Office
Engineering Directorate
MOL Systems Engineering Office

The information in a Technical Operating Report is developed for a particular program and is therefore not necessarily of broader technical applicability.

ABSTRACT

A model is developed for sliding and rolling friction that can be used in simulations of dynamic systems involving mechanical elements that are subject to friction. Sound bases for the model are developed around the hypothesis that the origin of friction is in quasi static contact bonds that are continuously formed and subsequently broken. Sliding friction, including coulomb friction and the so-called "stiction," as well as rolling friction are believed to be realistically simulated by the model. The model has been proven to accurately simulate transient torque and rate measurements on ball bearings tested in the laboratory.

I. INTRODUCTION

Recently, a series of ball bearing tests were conducted by H. Shibata in the Aerospace Corporation's Guidance and Control Laboratory under the direction of D. J. Griep. In discussions, Mr. Griep described to the author in detail the dynamical behavior of a simple experiment with three balls on a flat plate with another plate on top the three balls. His description clearly indicated that small displacements of the balls from a rest position caused an elastic restoring force on the balls. This deduction was obvious from the observation of lightly damped lateral oscillations about the rest position when the balls were disturbed. Discussions also encompassed the stochastic nature of rolling friction which the Aerospace tests were largely concerned with.

Mr. Griep welcomed the offer of this author to attempt to model and simulate the quasi static and stochastic friction phenomena. The following report is the result of this relatively meager exposure to the world of experimental friction. In the search for a reasonably plausible simulation model that would fit the experiment observations, some latitude has been taken with fundamental concepts of materials properties that no doubt are quantum mechanical and electrodynamical in nature and so the readers forbearance in this respect is solicited.

II. A THEORY OF SOLID FRICTION

A solid friction simulation model is desired that will accurately represent the physical phenomena commonly referred to as static friction, coulomb friction, and rolling friction. The combined effects of static and coulomb friction are usually depicted as shown in Figure 1.

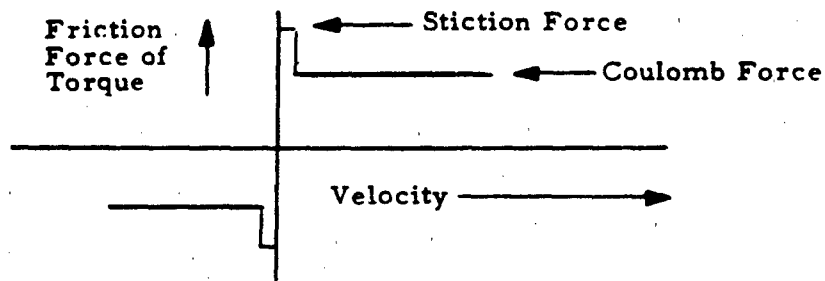


Figure 1. Conventional Representation of Solid Friction

Although generally accepted as a basic physical macro-phenomenon, coulomb friction may be explained on the basis of the quasi static properties of materials. Typically, these strength properties of solids appear as shown in Figure 2.

When a solid is stressed beyond its yield point the material undergoes permanent deformation and when the stress is removed the material behaves elastically; i.e., stress vs strain is linear during stress removal.

Usually, strain is thought of as being caused by an imposed stress. However, the reverse appears to be the convenient way to think of sliding friction between two solid bodies; i.e., stress or force or torque resisting the initial relative motion of the two solid bodies is caused by their relative

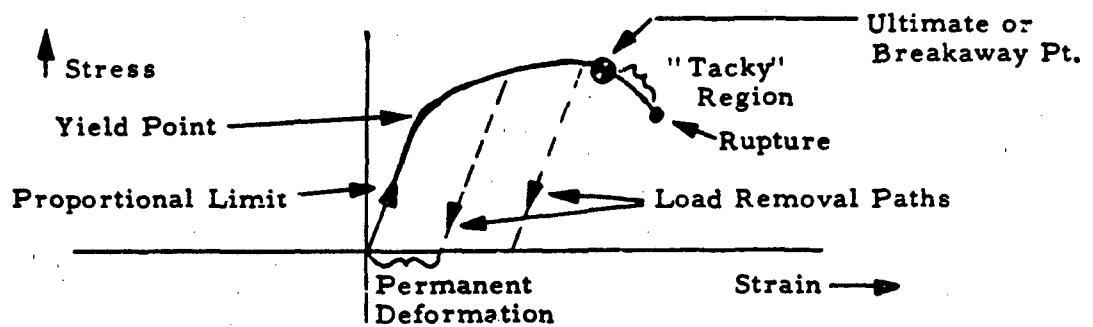


Figure 2. Strength Properties of Solids

motion that is brought about by an overpowering external force acting on the bodies. Thus, as strain or relative displacement of the bodies is increased, an internal restoring force proportional to this displacement is produced (considering the motion between the two bodies to be such that "breakaway" has not occurred so that the two bodies behave as one through the mechanism of partial cohesive bonding). Further relative displacement causes yielding or inelastic deformation of the solid materials at the bonding interface while the restoring force increases. A maximum restoring force is reached and, if the externally applied force is held constant, the two surfaces start to break free of each other during which time plastic deformation takes place while the two surfaces are still in solid "tacky" contact. Finally, rupture takes place and, if the two surfaces are not physically separated by some finite distance, the contacting elemental surfaces just ruptured will bond and break continuously with other elemental surfaces as this process proceeds.

This, then, is a description of what is called solid friction. It pertains to solids in contact without benefit of lubrication. The relationship of "stiction" and coulomb friction to this solid friction now becomes clear. The coulomb force is related to the interface bond rupture stress and the stiction force is related to the maximum or ultimate stress of the interface bond. Static friction or stiction and coulomb friction are seen to be indistinguishable in materials that exhibit brittle fracture properties as illustrated in Figure 3.

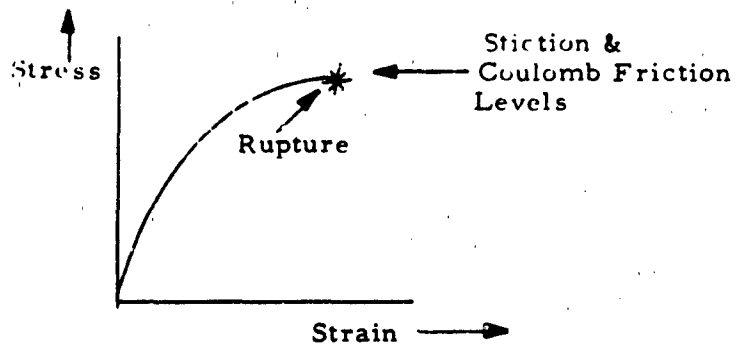


Figure 3. Brittle Material Failure Characteristic

Ductile materials can be expected to exhibit the stiction characteristic shown in Figure 4 where the "tacky" phase is encountered, which causes an essentially unstable progression from the point of maximum stress to the point of rupture. It is evident with this ductile material model, then, that it is possible for dynamic relaxation oscillations to exist in spring mass friction systems due to the negative slope portion of the stress-strain curve. It is this behavior that accounts for relaxation oscillation phenomena such as chatter, squeak, squeal, and stick-slip.

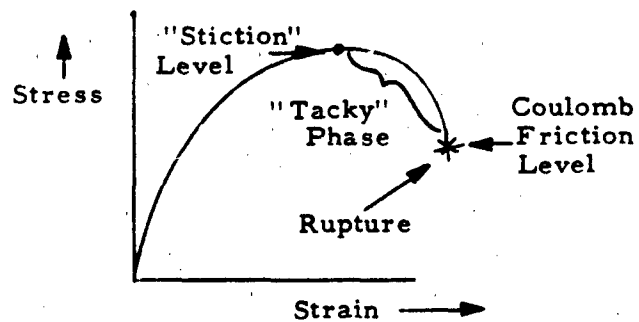


Figure 4. Ductile Material Failure Characteristic

It would seem too much to expect that the mechanism described above would apply equally well to both sliding and rolling friction, and yet it apparently does. Up to this point we have not made a distinction between sliding and rolling friction, and this was purposely done to imbue the idea that solid friction encompasses both of these types of friction. The difference between these types of friction may be explained simply by reference to Figures 5 and 6.

Figure 5 shows the case of sliding friction where the interface cohesively bonded regions undergo principally shearing stresses. Thus, the interface bond material properties that govern the sliding friction process are mostly their shear properties.

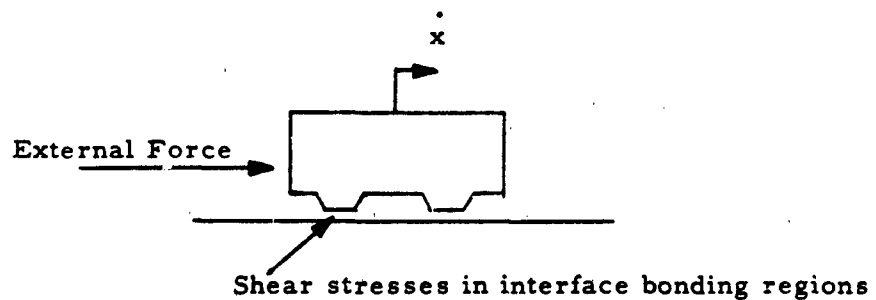


Figure 5. Sliding Friction

On the other hand, the case of rolling friction is illustrated in Figure 6 wherein the interface cohesively bonded regions are compressively stressed on the front side of the contact area and are stressed in tension on the back side. Thus, for rolling friction, tension and compression properties principally govern the friction process.

Sliding friction, then, involves shear failure because it is the only process by which continuous rupture can occur. Tensile failure would separate the bodies at rupture and compressive failure would break one or both of the bodies. Cutting of a solid material with a tool can be thought of as this kind of process, i. e., continuous shearing rupture.

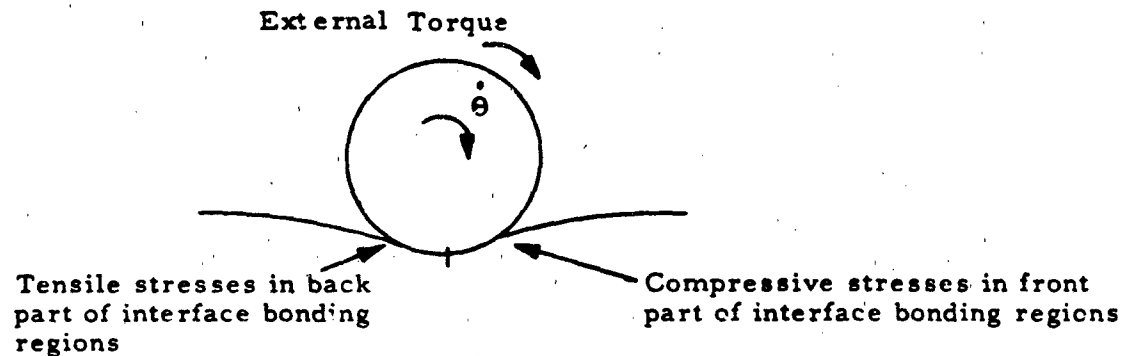


Figure 6. Rolling Friction

Rolling friction is seen to also involve continuous rupture, but the friction-associated rupture appears to be tensile in most engineering applications such as in ball bearings. Rolling mill crushers are an example of the continuous rupture process that involves continuous compressive failure. Ball bearings no doubt fail in compression when overloaded, but during normal operation the compressive stresses developed on the front side of the contact area merely helps establish the cohesive bond that must later be broken in tension on the back side of the contact area.

There is a question whether stiction, per se, can be distinctly identifiable in rolling friction. The author believes that it is not. This preconception is based on the notion that the interface bond strain is distributed over the area of contact where fracture occurs (i. e., the back side where tension failure proceeds) and thus an averaging of the strain over the stress-strain curve apparently takes place.

The physics of the continuous stress rupture process is not understood but conjecture leads this writer to believe that an explanation perhaps lies in Dorn's theory (References 4 and 5) that creep, leading to stress rupture, occurs in thermally activated deformation processes or perhaps vice versa, i. e., as in the friction-caused deformation process which induces thermal

activation and local interface heating. Thus, the back side bond creep rates being forced by rolling velocity are the result of contact bond energy of activation and entropy of activation produced by rolling compression on the front side. The entropy of activation is thus believed to be the thermal energy generated by the rolling friction process.

III. A SIMULATOR FOR SLIDING FRICTION IN DUCTILE MATERIALS

The process just described, coupled with Newton's second law, provides a model of solid sliding friction that can be represented by the schematic diagram of Figure 7. This process is simulated by the block diagram of Figure 8 where the net force available to accelerate the mass is the difference between the component of the external force parallel to the contacting surface elements and the frictional force. The time integral of the net force produces the velocity \dot{x} which is integrated to find the elemental displacement Δx from the initial equilibrium position. This elemental displacement is redefined each time the direction of motion changes. Thus, when relay R_3 in the diagram is activated by positive velocity, contact $R_{31}+$ is closed, and contact R_1 is closed prior to fracture, which permits integration to obtain the $+\Delta x$ relative displacement from the equilibrium position. When Δx reaches

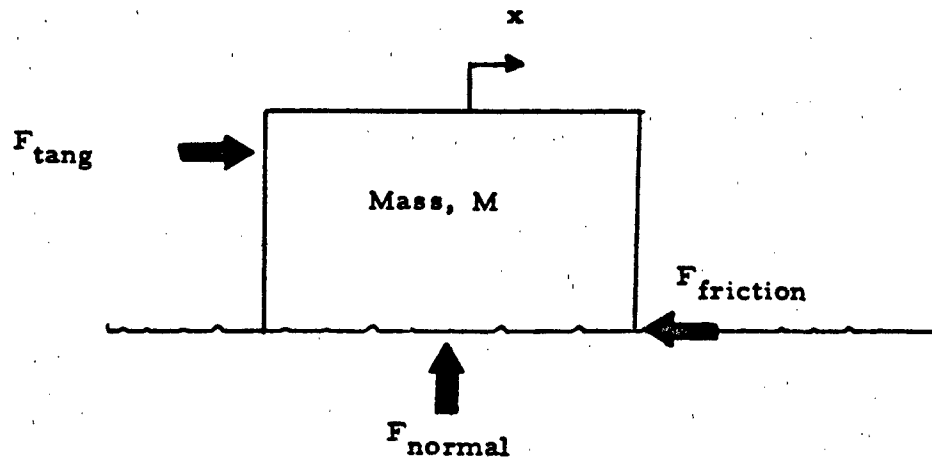


Figure 7. Dynamical Sliding Friction Model

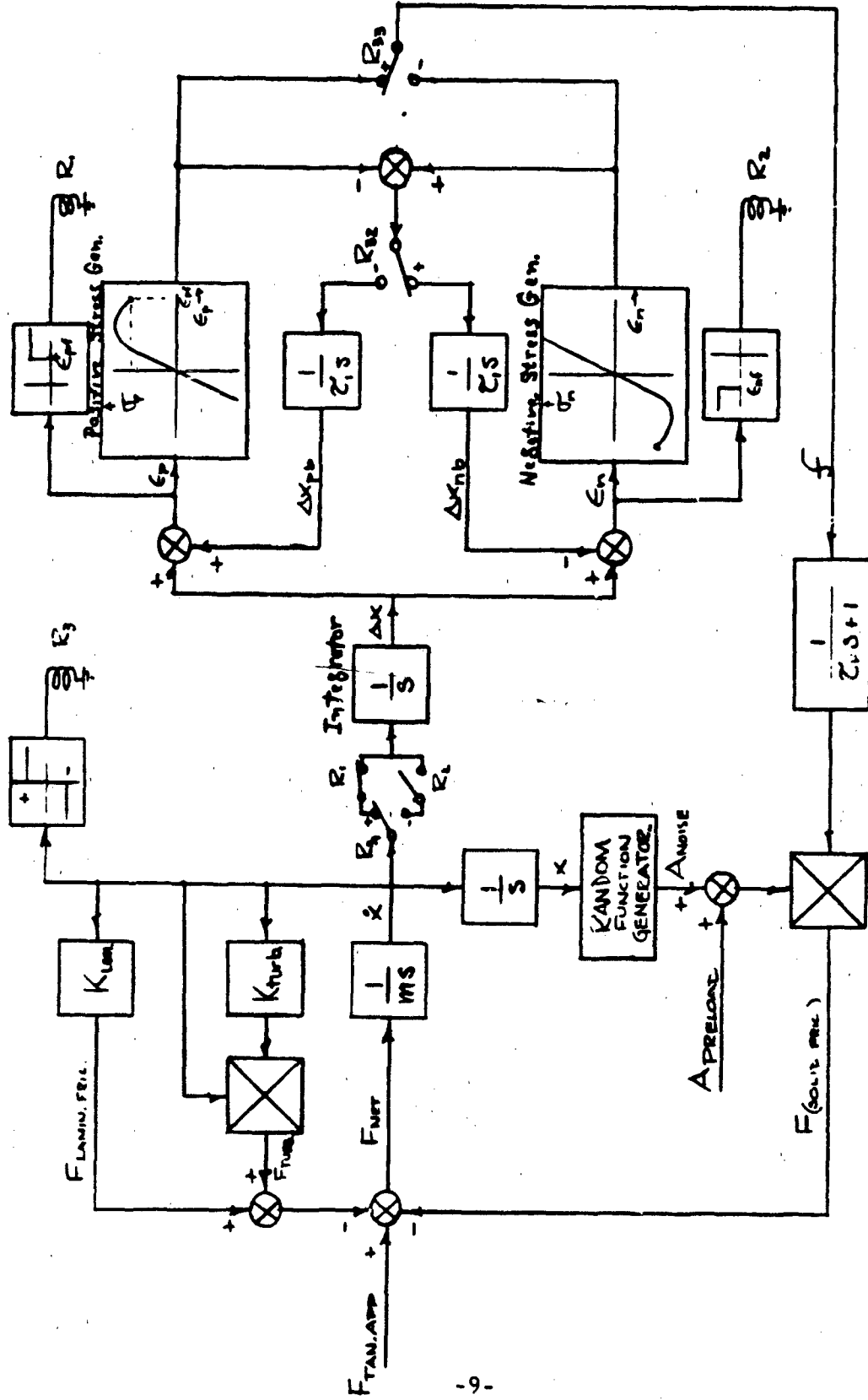


Figure 8. Solid Friction Simulator

ϵ_{pf} (assuming $\Delta x_{pb} = 0$), relay R_1 is actuated, corresponding to fracture of the contact bond, and the R_1 relay contact is opened thereby holding the value of Δx on the integrator output. The fracture level of stress is then filtered and multiplied by the contact area to obtain the net solid frictional force. This force is obviously constant as long as \dot{x} is positive and fracture has occurred and is seen to correspond to the coulomb friction force.

If the applied force is reversed, \dot{x} will change sign causing closure of the R_{31} - contact. The R_2 contact will be closed, because ϵ_n will be positive, corresponding to the establishment of the contact bond in the reverse direction. Thus, Δx will start to decrease from the value $\Delta x = \epsilon_{pf}$.

For $\dot{x} < 0$, the R_{33}^+ contact is opened and the R_{33}^- contact closed so that the friction level is set by the negative stress function σ_n . At the instant of \dot{x} reversal, $\sigma_n = \sigma_p$ due to the fact that σ_n is slaved to σ_p by servo action; i.e., σ_n is compared to σ_p and any error is integrated to bias the input to the negative stress function generator so as to drive the error between σ_n and σ_p to zero. It may be noted that the positive stress function σ_p is slaved to σ_n for negative motions ($\dot{x} < 0$) when σ_n is being read out to generate F_{solid} . Relay switching with contacts R_{32} and R_{33} is necessary to implement the load removal characteristic shown in Figure 2. A filter with time constant τ_F is added in the simulator to filter the R_{33} switch transients.

The net friction level is proportional to the load normal to the surface in the case of static and coulomb friction. The exact mechanism of this relationship is not understood fully and so, for the purposes of simulation, it is assumed that the contact or bond area is proportional to the force normal to the surface. Thus, $A_{preload}$ in the block diagram represents this force.

By multiplying the stress by area to obtain the frictional force, it becomes possible to introduce friction noise in what is believed to be a realistic manner. The area noise, A_{noise} , is that contact area variation produced by surface irregularities. It is a stochastic function of the variable x and so a random function generator is shown that generates $A_{noise}(x)$ for this purpose.

Laminar (viscous) and turbulent friction terms have been included in the simulator block diagram for generality. Laminar friction is assumed to be proportional to velocity, and turbulent friction is assumed to be proportional to the square of velocity.

IV. A SIMULATOR FOR SOLID FRICTION IN BRITTLE MATERIALS

An alternate and much simpler friction simulator than that in Figure 8 is shown in Figure 9. This simulator should be applicable to rolling friction and brittle dry sliding friction and perhaps to lubricated sliding friction involving ductile materials. In this simulator, advantage is taken of the observation that the friction stress function, f , being a function of displacement, x , can be differentiated with respect to time

$$\frac{df}{dt} = \frac{df}{dx} \cdot \frac{dx}{dt} = f' \dot{x}$$

and the result integrated to generate f . It is observed that f' is easily found as a function of x . The simulation block diagram, however, shows f' being generated using a function generator with f as the input. Thus it is required to determine f' as a function of f . This determination can be illustrated with a few examples.

Example 1

Assume $f(x) = kx, \quad -x_s < x < x_s$

or $f(x) = kx_s, \quad |x| > x_s$

Then $f' = k, \quad -x_s < x < x_s, \quad -kx_s < f < kx_s$
 $= 0, \quad , \quad |f| > kx_s$

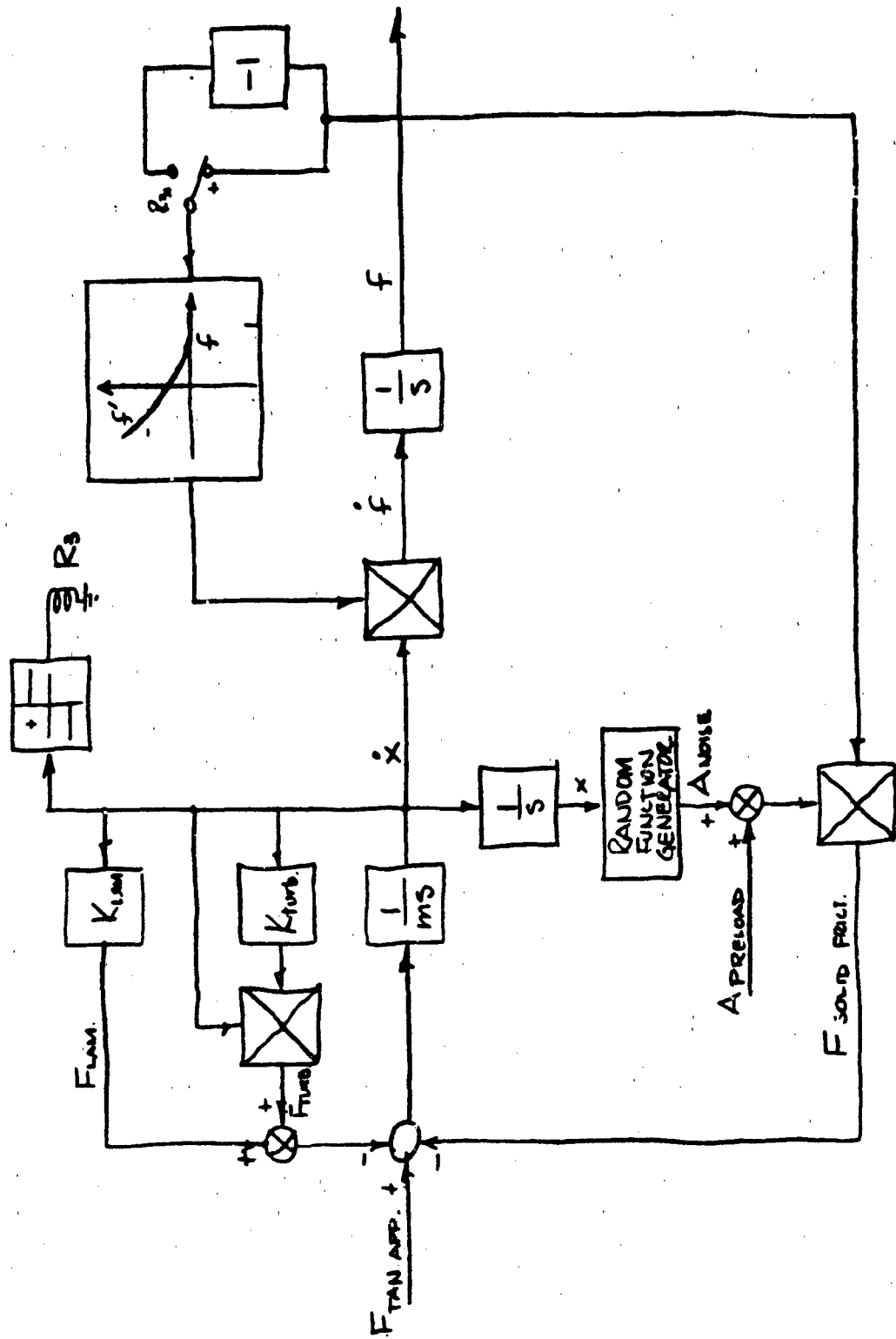
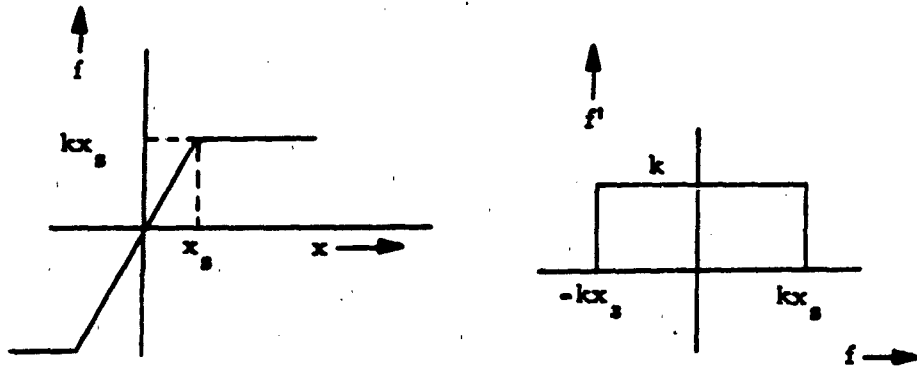


Figure 9. Friction Simulator For Sliding or Rolling Plus Fluid Friction

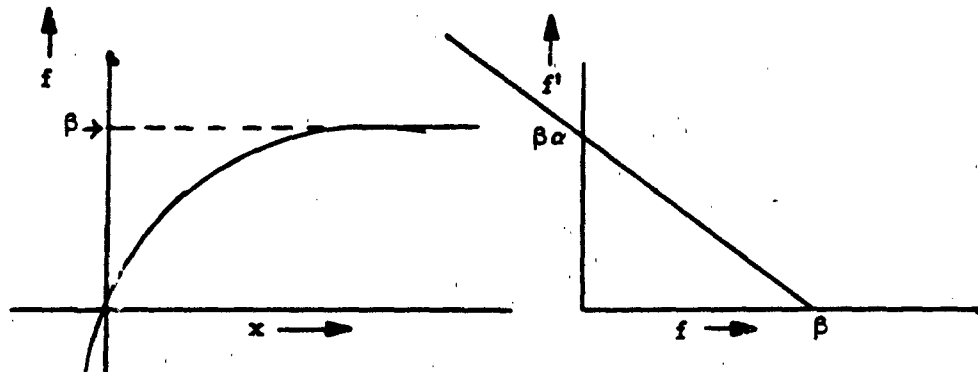
These relations are illustrated below:



Example 2

Assume $f(x) = \beta(1 - e^{-\alpha x})$, $x > 0$

Then $f' = \beta \alpha e^{-\alpha x}$
 $= \beta \alpha - \alpha f$ $f > 0$
 $f' > 0$



Example 3

Assume instead of a linear f' vs f relation as in Example 2, a square law relation

$$f' = \frac{df}{dx} = \gamma(f - f_0)^2$$

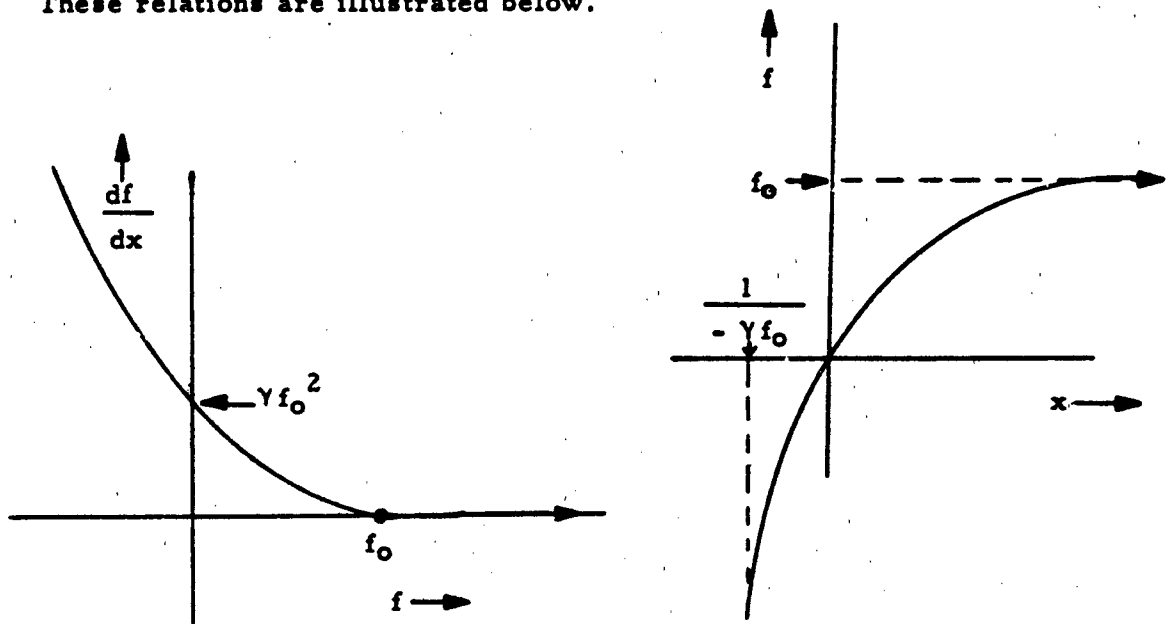
This is easily integrated to obtain

$$x + c = - \frac{1}{\gamma(f - f_0)}$$

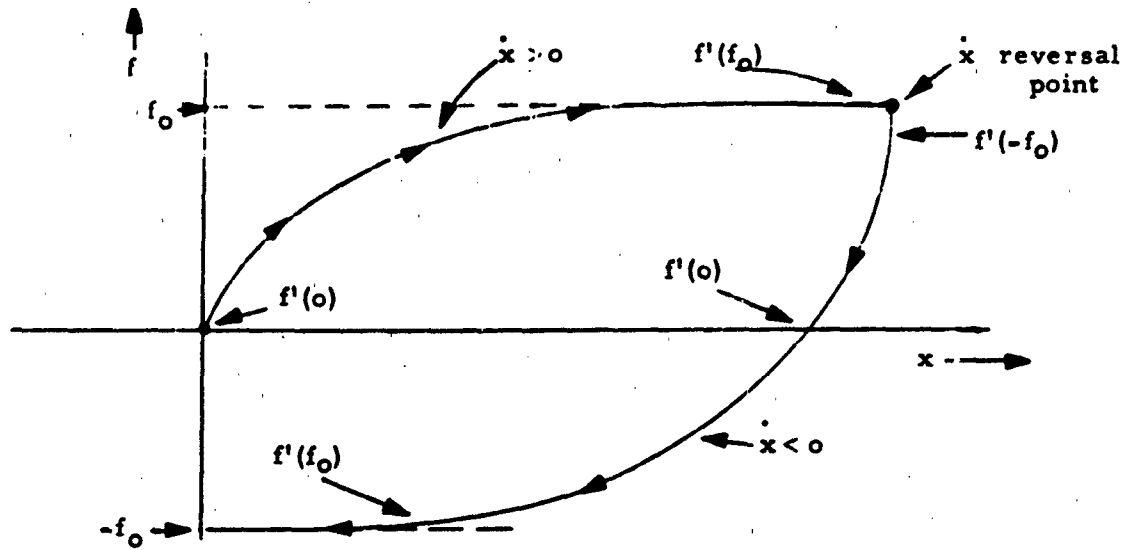
The constant of integration is determined by knowing that the friction $f = 0$ when at rest at $x = 0$. Thus, $c = 1/\gamma f_0$ and we obtain

$$f = \frac{\gamma f_0^2 x}{(\gamma f_0 x + 1)}$$

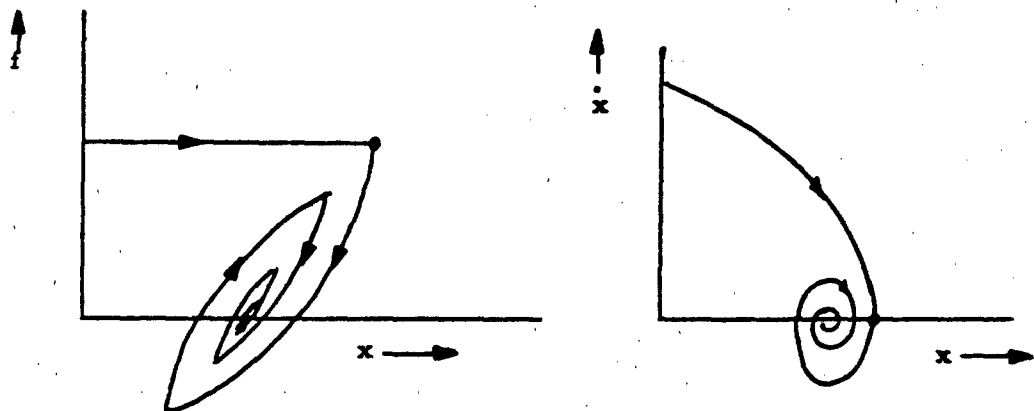
These relations are illustrated below.



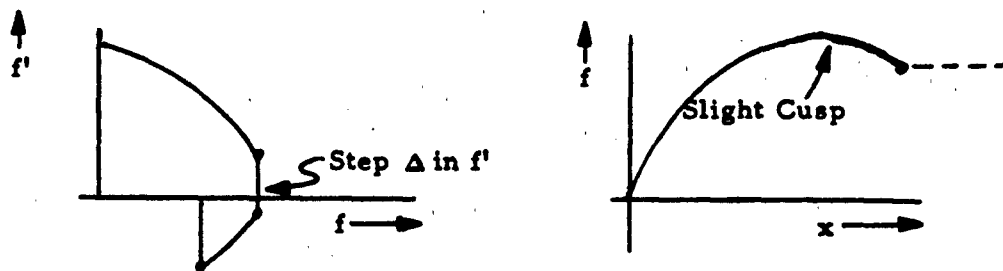
Referring to Figure 9, the time derivative of the friction function f is integrated to obtain $f(x)$. Starting at $x = 0$, $f = 0$, and for $x > 0$, it may be seen that $f(x)$ asymptotically approaches f_0 as indicated below. When \dot{x} changes sign and the direction of motion changes, relay R_3 is actuated thereby switching R_{31} . This changes the sign of f from $+$ to $-$ causing the value of f' to change from $f'(f)$ to a value $f'(-f)$. This behavior is exhibited for all levels of friction.



An illustrative example of the model is the case of the freely rolling ball on a flat surface with an initial velocity. The friction-displacement and phase plane trajectories are shown below.



Reflecting upon the examples above, one sees that the technique of generating f fails for double-valued functions, provided f' is required to be continuous; i.e., the integrator becomes stuck as f' passes through zero. This might be circumvented by intentionally placing a discontinuity in f' where it passes through zero as is illustrated below:



However, the simulator appears to be incapable of producing double-valued functions with diode function generators, and so only monotonic functions can be simulated with this type of equipment. It is believed at this time that monotonic functions will adequately represent rolling friction but not the so called static friction associated with sliding.

Since monotonic functions appear to be suited to simulation by the diagram of Figure 9, the characteristic limiting of f when $f' = 0$ is used to great advantage. For example, in rolling friction, \dot{x} can continue to persist and x will increase indefinitely while f is limited.

V. SIMULATION RESULTS

A computer simulation of the simple model shown in Figure 9 was implemented on an EAI TR-10 Analog Computer. The computer diagram used is shown in Figure 10. Experimental data on a 60 mm bore Class 7 super precision 12-degree contact angle ball bearing with a 60 lb preload was obtained by Hiro Shibata in the Aerospace Guidance and Control Laboratory under the direction of Dave Griep. The experimental apparatus was set up to drive the inner race of the ball bearing with a torquer whose current was closed-loop servo-controlled to maintain highly accurate angular rates which were measured with a gyro. The rate could be commanded, and several tests were run with sinusoidal input rates. Bearing friction torque was measured with a high accuracy Micro Gee position table adapted for use as a torque measuring instrument. The measured friction torque and gyro rate were recorded for four sinusoidal inputs to the rate drive servo. The frequencies of these four runs were 0.5, 0.1, 0.04, and 0.01 cps and the angular rate amplitude was 0.125 deg/sec in all four of these runs. The recorder trace data was reduced, and friction torque T_f was plotted versus angular displacement Θ which was computed using gyro data. The slopes of the resulting curves were measured to obtain $dT_f/d\Theta$ information that could be plotted versus T_f . The resulting test data is in Figure 11. Also shown in the figure is the function approximated by the DFG in the TR-10 simulation.

It is interesting to note that experimental data indicates a square law T' vs T relation. An empirical curve fit equation is also shown in Figure 11 for this data. The empirical equation determined is:

$$\frac{dT}{d\Theta} = \gamma(T - T_0)^2$$

where

$$\gamma T_0^2 = 36 \text{ in-oz/deg}$$

$$T_0 = 6 \text{ in-oz}$$

$$\gamma = 1.0 (\text{in-oz-deg})^{-1}$$

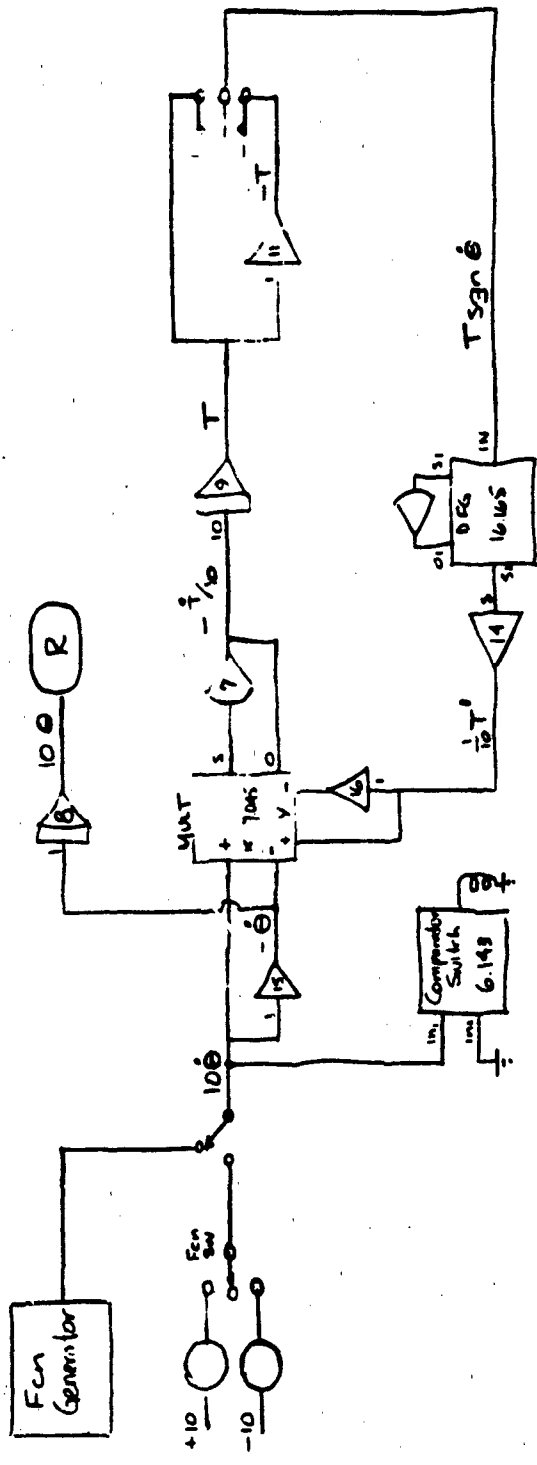


Figure 10. EAI TR-10 Analog Computer Diagram

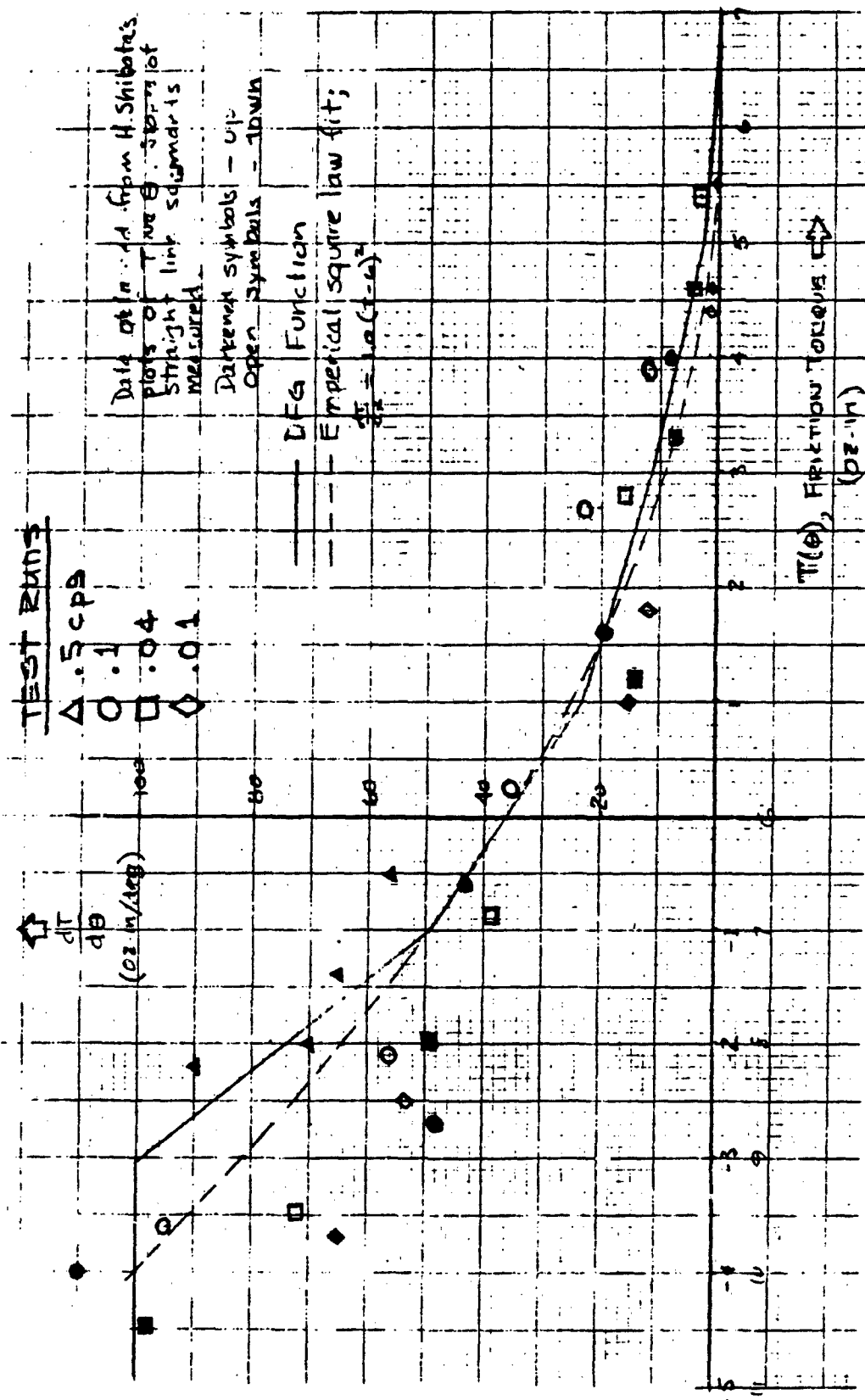


Figure 11. Experimental Data and Function Fit of $\frac{dT}{d\theta}$ vs τ

Simulation runs were made employing constant rate $\dot{\theta}$ inputs to the simulator and other input functions such as sawtooth and sine functions. Because it had been expected that the experimental test results could be interpreted according to the coulomb friction model, the data obtained from the tests were plotted as friction torque versus angular rate. Accordingly, several runs were made simulating the tests and the computer torque and rate variables were recorded on an x-y plotter.

Results of the simulation are shown in Figure 12. For comparison, the experimental data are shown for half of a cycle for each frequency.

The validity of the model presented here can hardly be disputed on the basis of this and other comparisons that have been made. The comparison of Figure 12 shows that the simulation faithfully reproduces the unexpected hysteresis characteristic first noted by H. Shibata. It is apparent by examination of Figure 12 that, as frequency is lowered, the step-like nature of coulomb friction is approached with the width of the hysteresis loop reduced. In the limit, as frequency goes to zero, the step-like discontinuity is approached and the hysteresis loop width will vanish. Thus we see that coulomb friction is a special case of the more general solid friction model presented here.

It is interesting to speculate that the friction model developed here is applicable to magnetic and other forms of hysteresis. Physical processes that exhibit hysteresis are now believed to be characterized by the functional dependence of the ordinate variable on the time integral of the abscissa variable. The resulting functions behave as a brush whose bristles must bend as the brush moves in one direction and then flop or bend in the opposite direction if the motion is reversed.

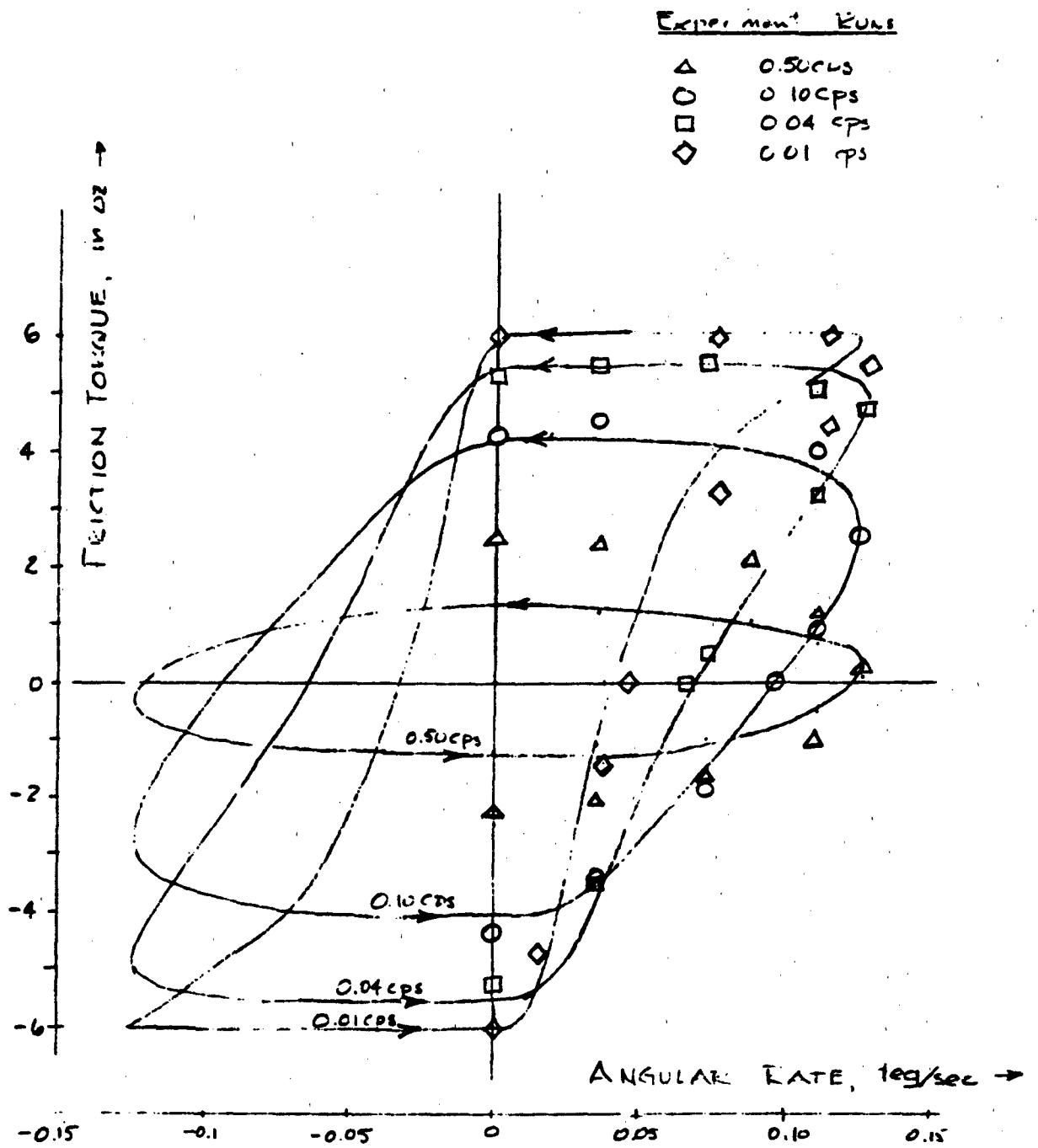


Figure 12. Comparison of Simulator and Experimental Test Results

VI. CONCLUSIONS

A general model for solid friction has been presented that has been validated by ball bearing friction experiments data.

The heretofore unexpected hysteresis characteristic in rolling friction found by Shibata and Griep was somewhat amazingly simulated by the simple computer simulation over a wide frequency range.

Coulomb friction was found to be a special case of the general solid friction model.

Static friction (stiction) is exhibited during sliding between ductile materials.

Stiction does not occur in sliding between brittle (or well lubricated) materials. It is speculated that stiction is rare or completely absent in rolling friction.

Rolling friction involves a compressing/tensing process and sliding involves a shearing process.

Solid friction is caused principally by contact bond stress and is quasi static in character. Making and breaking of the contact bonds is dynamic and governed by motion of the bodies driven by the external or inertial forces.

The friction model presented is believed to be related theoretically to magnetic hysteresis and the simulator described can obviously be used to simulate other forms of hysteresis.

The stochastic nature of various forms of friction is thought to enter through the randomness of contact area variation and a seemingly plausible way of including this in the simulation model is shown. However, the accuracy of this representation has yet to be validated. Analog computer random function generators are not available that directly produce functions of variables other than time, and so a digital simulator might be more applicable for this purpose.

REFERENCES

1. Polakowski, N. H., and Ripling, E. J., Strength and Structure of Engineering Materials, Prentice Hall, Englewood Cliffs, New Jersey, 1966.
2. Rabinowicz, E., Friction and Wear of Materials, John Wiley, 1965.
3. Korn, G., "A New Analog Computer Setup for Simulation of Static and Coulomb Friction," Inst. & Control System (Sept 1962), pg 171.
4. Kennedy, A. J., Processes of Fatigue and Creep in Metals (pp 215-228), Oliver and Boyd, Edinburgh, 1962.
5. Am. Soc. Metals, "Creep and Recovery," (pp 225-283), Cleveland, 1957.
6. Bisson, E. B. and Anderson, W. J., Advanced Bearing Technology, NASA Doc SP-38, 1964.